

9126

NACA TN 2765



# NATIONAL ADVISORY COMMITTEE FOR AERONAUTICS

TECHNICAL NOTE 2765

A FLIGHT INVESTIGATION OF THE EFFECT OF SHAPE AND  
THICKNESS OF THE BOUNDARY LAYER ON THE PRESSURE  
DISTRIBUTION IN THE PRESENCE OF SHOCK

By Eziaslav N. Harrin

Langley Aeronautical Laboratory  
Langley Field, Va.



Washington

September 1952

AFMDC

TECHNICAL LIBRARY  
AFL 2011



## NATIONAL ADVISORY COMMITTEE FOR AERONAUTICS

## TECHNICAL NOTE 2765

A FLIGHT INVESTIGATION OF THE EFFECT OF SHAPE AND  
THICKNESS OF THE BOUNDARY LAYER ON THE PRESSURE  
DISTRIBUTION IN THE PRESENCE OF SHOCK

By Eziaslav N. Harrin

## SUMMARY

An investigation was made in flight at free-stream Mach numbers up to about 0.77 to determine the effect of a laminar boundary layer and thin and thick turbulent boundary layers on the chordwise pressure distribution over an airfoil in the presence of shock at full-scale Reynolds numbers. Boundary-layer and pressure-distribution measurements were made on a short-span airfoil built around the wing of a fighter airplane. Boundary-layer Reynolds numbers (based on momentum thickness and flow parameters at the outer edge of the boundary layer) were about 3,000 for the laminar boundary layer and 10,000 for the thickest turbulent boundary layer with local Mach numbers ranging up to 1.3 and chord Reynolds numbers up to about  $21 \times 10^6$ .

The results indicated very little difference in pressure distribution with laminar and turbulent boundary layers extending up to the position of shock. The principal difference was a 2- to 3-percent-chord more forward position of the pressure rise at the surface with the turbulent boundary layers. Other investigations made at low Reynolds numbers (of the order of  $3 \times 10^6$ ) indicated large pressure differences extending over an appreciable extent in the chordwise direction.

## INTRODUCTION

The interaction of shock with laminar and turbulent boundary layers at low Reynolds numbers (up to about  $3 \times 10^6$ ) has been investigated in detail in recent years (refs. 1 to 5). These investigations, and particularly that of reference 1, indicated such a large difference in pressure distribution with laminar and turbulent boundary layers that an airfoil under these conditions would be expected to experience appreciably different forces and moments. At high or full-scale

Reynolds numbers, no corresponding information was available on boundary-layer—shock interaction. In order to provide some information at full-scale Reynolds numbers up to about  $20 \times 10^6$ , an investigation, reported herein, was initiated on a short-span airfoil built around the wing of a fighter airplane.

The purpose of this paper is to present some measurements of pressure distribution obtained in flight at Reynolds numbers from  $17.5 \times 10^6$  to  $21.2 \times 10^6$  with laminar and turbulent boundary layers extending to the position of shock. These measurements were made in dives up to a flight Mach number of 0.766 which was sufficiently high to give extensive regions of local supersonic flow.

### SYMBOLS

$R_c$	Reynolds number based on free-stream conditions and chord of airfoil
$R_\theta$	boundary-layer Reynolds number based on local condition immediately outside boundary layer and on momentum thickness, $u_\delta \rho_\delta \theta / \mu_\delta$
$\delta^*$	displacement thickness, $\int_0^\delta \left(1 - \frac{\rho u}{\rho_\delta u_\delta}\right) dy$
$\theta$	momentum thickness, $\int_0^\delta \frac{\rho u}{\rho_\delta u_\delta} \left(1 - \frac{u}{u_\delta}\right) dy$
$u$	velocity in boundary layer in x-direction
$\rho$	mass density in boundary layer
$\rho_o$	free-stream mass density
$M$	Mach number
$V_o$	free-stream velocity
$q_o$	free-stream dynamic pressure, $\frac{1}{2} \rho_o V_o^2$
$p$	static pressure
$P$	pressure coefficient, $\frac{p_\delta - p_o}{q_o}$

$p_T$	total pressure
$x$	chordwise distance from leading edge along surface of test airfoil or curved plate
$y$	distance perpendicular to surface of test airfoil
$l$	length of supersonic region with turbulent flow in boundary layer
$C_L$	airplane lift coefficient
$c$	airfoil chord
$\mu$	coefficient of viscosity
Subscripts:	
$\delta$	outer edge of boundary layer
$o$	free stream

#### APPARATUS AND TESTS

Boundary-layer and pressure-distribution measurements were made on a short-span airfoil built around the wing of a fighter airplane. This test airfoil had a chord of 89.0 inches, a span of 60 inches, and a maximum thickness of 16 percent chord. The airfoil section was approximately an NACA 64-series section. The test airfoil was constructed of laminated wood and covered with a  $\frac{1}{8}$ -inch-thick sheet of aluminum to provide a smooth and stable surface. Actually two airfoils were built and one was mounted on each wing. Only one of the airfoils was used for the measurements; the other was used to provide lateral balance to the airplane. A photograph showing the airplane with the test airfoils prior to being covered with the aluminum sheet is presented as figure 1.

Static-pressure orifices were installed on the upper surface at 35 percent chord and every  $2\frac{1}{2}$  percent chord from  $42\frac{1}{2}$  to 65 percent chord. Each orifice consisted of a slit 0.6 inch long (spanwise) and 0.003 inch wide (chordwise) followed by a small plenum chamber and tubing which led to the pressure recorder. This special shape of orifice was used in an effort to minimize any adverse effect on the laminar boundary layer of flow in or out of the orifice resulting from variations of pressure at the orifice associated with varying speed and altitude.

Total-pressure measurements through the boundary layer were made with boundary-layer rakes consisting of eight total-pressure probes. These probes were made of stainless-steel tubing of 0.06-inch inside diameter and 0.015-inch wall thickness with the upstream end of each tube flattened and filed into a rectangular opening 0.003 inch high and 0.1 inch long with a wall thickness of about 0.003 inch.

The boundary-layer rakes were used in pairs at 50 and  $52\frac{1}{2}$  percent chord in some tests and 55 and  $57\frac{1}{2}$  percent chord in others. The boundary-layer rakes were set about 1 inch on each side of the line of orifices in the spanwise direction (fig. 2). The heights of the tubes were checked before and after each flight.

All the measurements were made in dives which were started by "pushing over" at an altitude of 28,000 feet and a Mach number of 0.6 to a dive angle of  $38^\circ$  and continued until an airplane Mach number of 0.76 was reached, at which time a gradual pull-out was begun. Data were recorded from a Mach number of 0.6 up to the highest Mach number attained, which was approximately 0.77. Lift coefficients during the portion of the dives in which the measurements were made varied from approximately 0.16 to 0.08 at the high-speed end of the dive. The free-stream Reynolds number (based on the chord of the test airfoil section) range for these tests was from  $17.5 \times 10^6$  to  $21.2 \times 10^6$ .

Boundary-layer and static-pressure measurements were made with three surface conditions of the test airfoils: (1) smooth, (2) transition strip at 30 percent chord of the upper surface consisting of a spanwise strip of cellulose tape 1 inch wide and 0.003 inch thick, and (3) transition strip at 4 percent chord of the upper surface consisting of a 0.035-inch-diameter thread taped to the surface.

Free-stream total pressure  $p_{T_0}$  and static pressure were measured by means of a pitot-static tube mounted on a boom about 1 chord ahead of the airplane wing tip. The measured static pressures were corrected to free-stream static pressures  $p_0$ .

Pressures were measured with NACA recording multiple manometers. Normal acceleration used for determining airplane lift coefficient was measured by using an NACA air-damped recording accelerometer.

## RESULTS

Chordwise pressure distributions over the upper surface in the region of shock are shown in figures 3 and 4 for two flight Mach numbers ( $0.740 \pm 0.001$  and  $0.766 \pm 0.002$ ) and three surface conditions. The distribution of Mach number through the boundary layer, determined from measurements of total pressure through the boundary layer and static pressure at the surface, is also shown in figures 3 and 4. These boundary-layer profiles were selected for chordwise positions as close to the position of shock as were available. Boundary-layer Reynolds numbers based on momentum thickness and flow parameters at the outer edge of the boundary layer were about 3,000 for the laminar boundary layer, 8,000 for the turbulent layer with transition strip at 30 percent chord, and 10,000 for the turbulent layer with the transition strip at 4 percent chord.

Since the pressure-distribution measurements for each surface condition were made in separate flights, some uncertainty is involved in the comparison of pressure distributions selected for a given flight Mach number due to inaccuracy of determining Mach number. An estimate based on the accuracy of measurements of free-stream static and total pressures indicated that flight conditions could be matched with a probable accuracy in flight Mach number of  $\pm 0.005$ . This error in Mach number is estimated to correspond to a change in the position of shock (which varies with Mach number) of no more than  $1\frac{1}{2}$  percent chord. The contribution of such a change in position of shock to the indicated pressure differences is therefore small.

Another factor which affects the comparison is the lag of the pressure measuring system. The tests, as mentioned previously, were made in dives in which the Mach number was increasing and the position of shock was moving rearward. The large decrease in surface pressure as the shock passed over a given orifice caused the pressure at the orifice to lag by amounts depending on the time rate of shock passage over the orifice. For the flight conditions shown in figures 3 and 4, estimates indicated that the effect of lag due to shock passage over the orifices on the pressure measurements was within 5 percent of free-stream dynamic pressure for most of the orifices within the pressure rise, except at 55 percent chord (fig. 3) with the transition strip at 30 percent chord where the lag was estimated to be about 15 percent dynamic pressure.

The pressure distributions shown in figures 3 and 4 for the different boundary-layer conditions are at somewhat different airplane lift coefficients. Examination of other data obtained at a given Mach number over a greater range of lift coefficient than those of figures 3 and 4 indicated that the comparison of pressure distributions in

figure 3 should be unaffected by the small differences in lift coefficient.

The possibility also exists that the pressure distributions measured were affected somewhat by the presence of the boundary-layer rakes. The magnitude of any such effect is not known.

The distribution of Mach number through the boundary layer as shown in figures 3 and 4 is intended mainly to indicate the nature of the boundary layer immediately ahead of the shock. Because of the high sensitivity of Mach number or velocity next to the surface to small errors (such as those due to measurement or lag), the distribution near the surface is probably only qualitative. The indicated separation for laminar flow in figure 3 should be regarded in this manner. The value of the local Mach number for the same tube position in figure 4 appears to be too high although no explanation for this phenomenon can be given. The distribution of Mach number through the boundary layer in figure 4 for the condition with a transition strip of 4 percent chord was extrapolated to the edge of the boundary layer on the basis of a power profile fitted to that part of the boundary layer over which measurements were available.

Since the present results were obtained at high Reynolds numbers, a comparison with the low Reynolds number results of reference 1 is desirable. A direct comparison of the results on the basis of wing chord as the characteristic length, however, was not possible inasmuch as the data of reference 1 were obtained on a curved plate in a wind tunnel. An analysis of the data with turbulent flow indicated that, if the length of the local supersonic region was used as the characteristic length, the pressure distributions for the tunnel and flight tests were very similar for about the same maximum local Mach number. This characteristic length was therefore used as a basis for comparison to indicate differences in pressure distributions with laminar and turbulent flow for the low and high Reynolds numbers. Such a comparison is made in figure 5, together with a comparison of the actual distributions of Mach number through the boundary layer. (The pressure distribution ahead of 35 percent chord or chord of  $\frac{x}{l} = 0.335$  for the flight results was obtained from other tests in which orifices up to the leading edge were used. These data are presented only to determine the length of the local supersonic region for flight tests.) A scale of local Mach number  $M_\delta$ , corresponding to the scale of pressure ratios  $p/p_T$  on the left-hand side of figure 5(a), is shown on the right-hand side of the figure for the convenience of the reader.

## DISCUSSION

The results in figures 3 and 4 indicate very little difference in pressure distribution with laminar and turbulent boundary layers ahead of the shock. The position of shock as evidenced by the pressure rise is slightly farther forward (2 to 3 percent chord) with the turbulent layers than with the laminar layer and the pressure gradient is not quite so steep. A large part of the small differences in pressures ahead and behind the pressure rise is probably within experimental error.

The comparison in figure 5 shows that the differences in pressure distribution with laminar and turbulent boundary layers ahead of the shock are considerably greater at low Reynolds numbers (about  $3 \times 10^6$ ) than at the full-scale Reynolds numbers of the present tests (about  $21 \times 10^6$ ). The flattening and reduction of the pressure peak for the laminar boundary layer of the low Reynolds number tests of reference 1 were shown to be associated with separation due to the forward propagation of pressure through the laminar boundary layer from the high-pressure region behind the shock. No separation was in evidence in the tests with turbulent flow. In the present tests, the relatively thinner laminar boundary layer limited the extent to which the pressure rise due to the shock could influence the surface pressures upstream of the shock. Although there is evidence that separation occurred in some of the high Reynolds number tests (for conditions not presented herein) with the laminar boundary layer, it occurred too close to the shock to have a large influence on the pressure distribution as compared with the turbulent case. From unpublished data obtained in a blowdown jet in the Langley Gas Dynamics Branch, the change in pressure distribution due to laminar separation at the Reynolds numbers of the present tests has been indicated to correspond to a change in pressure coefficient of about 0.007. Such a change would obviously be obscured by pressure lag and other experimental inaccuracies of the present tests. As a result of the large differences in pressure distribution that occur at low Reynolds numbers, an airfoil at low Reynolds numbers would be expected to experience greater differences in forces and moments with the different types of boundary layers than an airfoil at high Reynolds numbers.

## CONCLUSIONS

In the flight investigation made to determine the effect of the type of boundary layer ahead of the shock on the pressure distribution over an airfoil at Mach numbers up to about 0.77 and a chord Reynolds number up to about  $21 \times 10^6$ , the results indicated very little difference in pressure distribution for laminar and turbulent boundary



layers extending up to the position of shock. The principal difference was a 2- to 3-percent-chord more forward position of the pressure rise at the surface with the turbulent boundary layers. Other investigations made at low Reynolds numbers (of the order of  $3 \times 10^6$ ) indicated large pressure differences extending over an appreciable extent in the chord-wise direction.

Langley Aeronautical Laboratory;  
National Advisory Committee for Aeronautics,  
Langley Field, Va., June 12, 1952.

#### REFERENCES

1. Ackeret, J., Feldmann, F., and Rott, N.: Investigations of Compression Shocks and Boundary Layers in Gases Moving at High Speed. NACA TM 1113, 1947.
2. Liepmann, H. W., Roshko, A., and Dhawan, S.: On Reflection of Shock Waves From Boundary Layers. NACA TN 2334, 1951.
3. Lees, Lester: Interaction Between the Laminar Boundary Layer Over a Plane Surface and an Incident Oblique Shock Wave. Rep. No. 143, Princeton Univ. Aero. Eng. Lab., Jan. 24, 1949.
4. Barry, F. W., Shapiro, A. H., and Neumann, E. P.: The Interaction of Shock Waves With Boundary Layers on a Flat Surface. Jour. Aero. Sci., vol. 18, no. 4, Apr. 1951, pp. 229-238.
5. Stewartson, K.: On the Interaction Between Shock Waves and Boundary Layers. Proc. Cambridge Phil. Soc., vol. 47, pt. 3, July 1951, pp. 545-553.

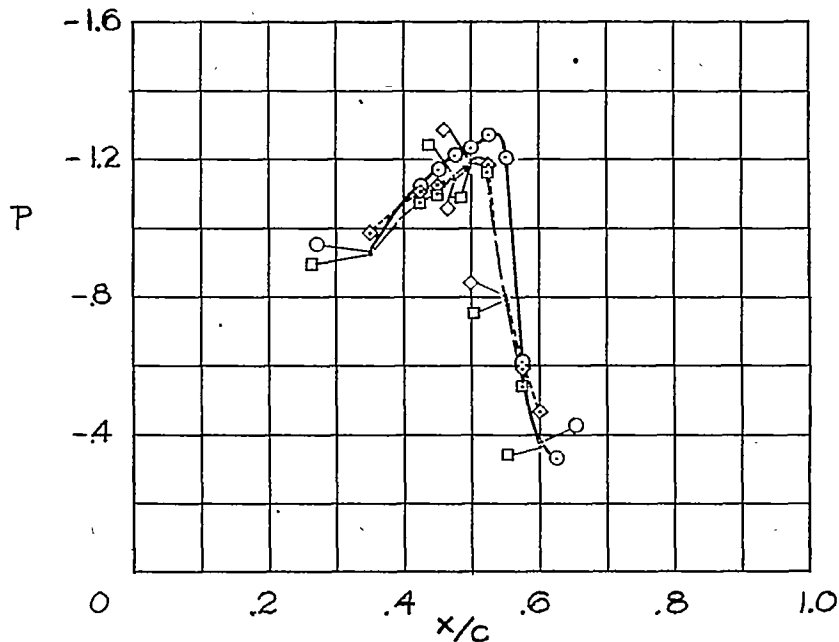


Figure 1.- Airplane with short-span airfoils installed on wings (prior to test surfaces being covered with aluminum sheets).



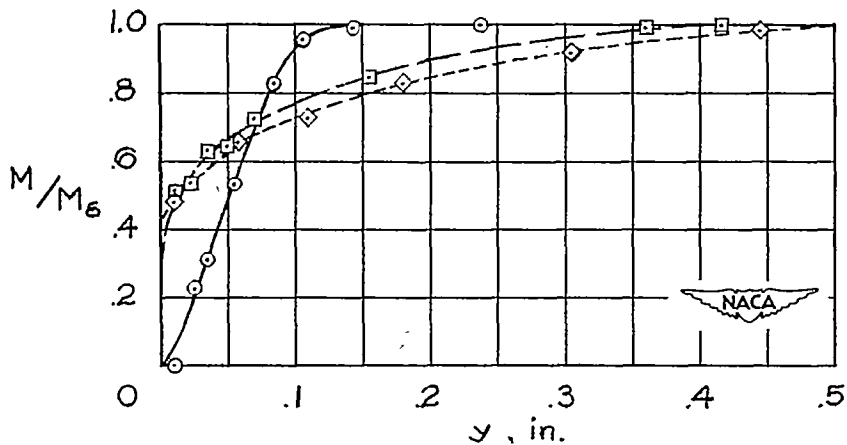
Figure 2.- Typical arrangement of boundary-layer rakes. Auxiliary static-pressure tubes and surface orifices are also shown.

NACA  
L-64246.1



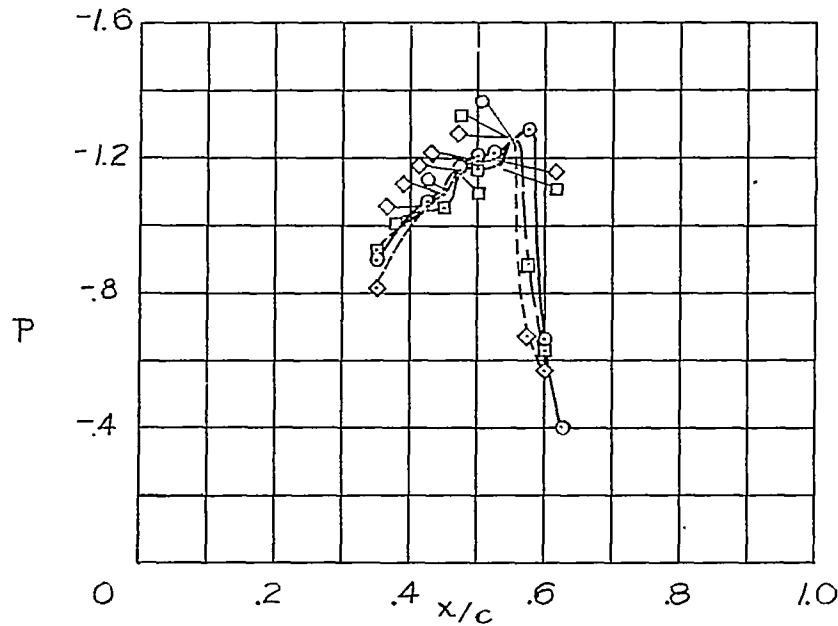
(a) Pressure distribution.

Transition strip, percent chord	Rake location, percent chord	$\delta^*$ , in.	$\theta$ , in.	$R_\theta$	$R_c$	
○	None	55	0.0475	0.0131	3,120	$18.9 \times 10^6$
□	30	$52\frac{1}{2}$	.0703	.0336	7,670	$18.0 \times 10^6$
◇	4	$52\frac{1}{2}$	.0949	.0459	10,250	$18.0 \times 10^6$



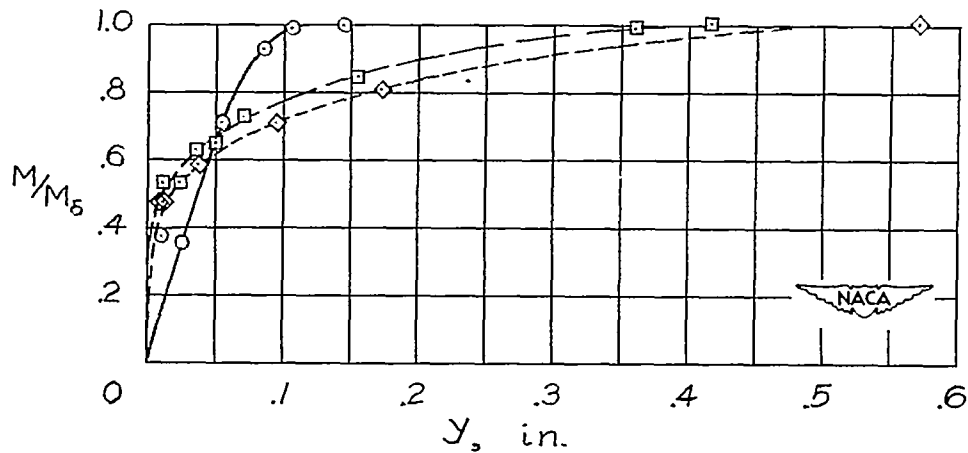
(b) Boundary-layer profiles.

Figure 3.- Chordwise pressure distribution over the upper surface for several boundary-layer conditions. Corresponding boundary-layer profiles immediately ahead of shock also shown.  $M_0 = 0.740 \pm 0.001$ ;  $C_L = 0.100 \pm 0.020$ .



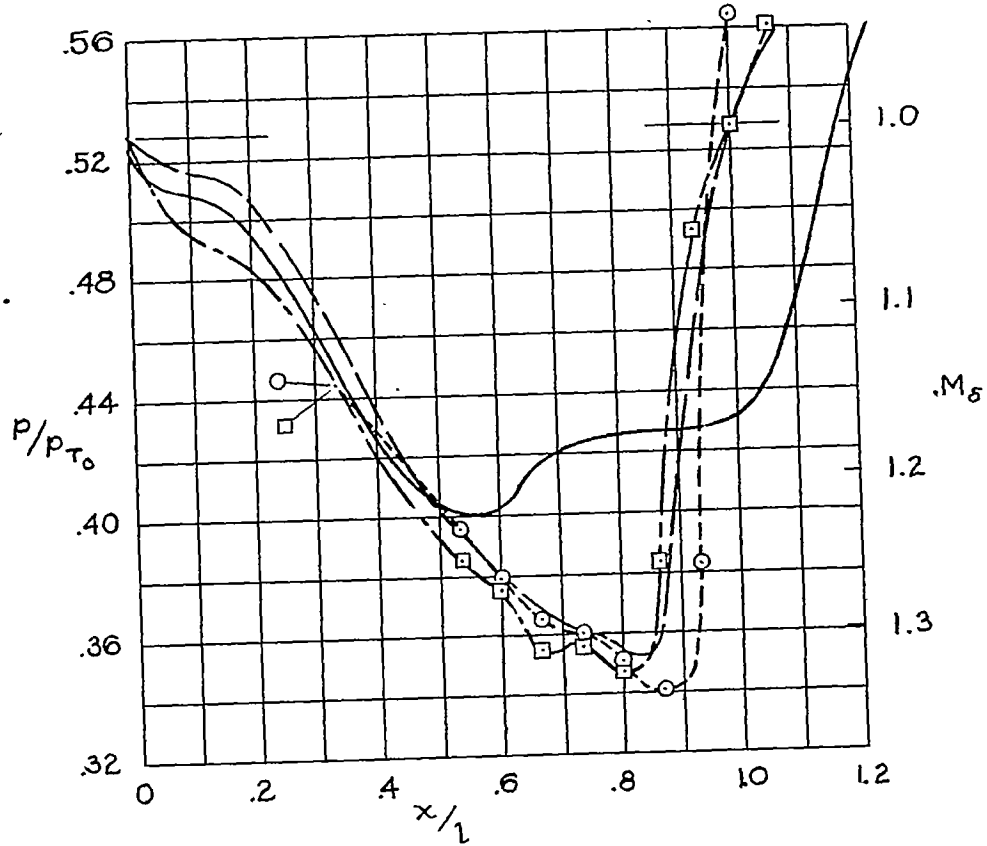
(a) Pressure distribution.

Transition strip, percent chord	Rake location, percent chord	$\delta^*$ , in.	$\theta$ , in.	$R_\theta$	$R_c$	
—○—	None	55	0.0436	0.0120	3,100	$21.2 \times 10^6$
—□—	30	$52\frac{1}{2}$	.0694	.0326	7,820	$18.9 \times 10^6$
---◇---	4	55	.0981	.0446	10,640	$19.5 \times 10^6$



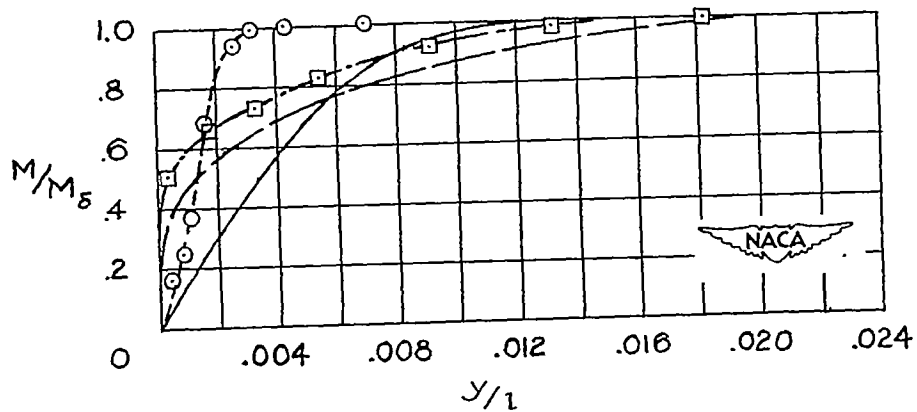
(b) Boundary-layer profiles.

Figure 4.- Chordwise pressure distribution over the upper surface for several boundary-layer conditions. Corresponding boundary-layer profiles immediately ahead of shock also shown.  $M_\infty = 0.766 \pm 0.002$ ;  $C_L = 0.085 \pm 0.015$ .



(a) Pressure distribution.

	$x/l$	$\delta^*/l$	$\theta/l$	$Re$	
---○---	0.866	0.00140	0.000332	2,770	Present data
---□---	.800	.00256	.00122	10,010	
---	.523	.00346	.00128	440	Reference 1 data
---	.711	.00381	.00168	1,478	



(b) Boundary-layer profiles.

Figure 5.- Comparison of pressure distribution in the neighborhood of shock with laminar and turbulent flow in the boundary layer at low and high Reynolds numbers. Boundary-layer data also shown.